Synthesis of Sulfur-Containing Polyacetylenes and Fabrication of Their Hybrids with ZnO Nanoparticles

Haipeng Xu,[†] Jia Ke Jin,[†] Yu Mao,[†] Jing Zhi Sun,*[,†] Feng Yang,[†] Wang Zhang Yuan,[†] Yong Qiang Dong,[†] Mang Wang,[†] and Ben Zhong Tang*[,†,‡]

Department of Polymer Science and Engineering, Zhejiang University, Hangzhou 310027, China, and Department of Chemistry, The Hong Kong University of Science & Technology, Clear Water Bay, Kowloon, Hong Kong, China

Received October 21, 2007; Revised Manuscript Received February 29, 2008

ABSTRACT: It has been a challenge to synthesize thiol-functionalized polyacetylenes because of the poisoning effect of mercapto group on the early transition-metal catalysts. Rhodium complexes such as $[Rh(cod)Cl]_2$ can catalyze the polymerizations but the products are insoluble and intractable. In this work, we tackled this challenge. Sulfur-containing polyacetylenes with macroscopic processability were successfully synthesized by separating thiol pendant from polyene backbone with a flexible spacer (in P**1**), capping free mercapto group with acetyl or alkyl group (in P**2** or P**3**), and using a zwitterionic complex $Rh^+[\eta^6\text{-}C_6H_5(nbd)B^-(C_6H_5)_3]$ as catalyst. The soluble polymers were characterized by NMR, IR, UV, PL, and TGA analyses. Due to the specific interactions between thiol group and zinc cation, ZnO nanoparticles were chemisorbed onto the surfaces of polymer films, as verified by AFM analysis. Polymer P**2** and ZnO nanoparticles could be readily hybridized by simply mixing the two components in an organic solvent such as chloroform, THF, or DMF. SEM images revealed that the morphology of the film cast from the solution of the P**2**/ZnO hybrid was dominated by well-dispersed nanoparticles and smooth surface.

Introduction

Hybridization of organic polymers with metal or semiconductor nanomaterials has attracted much interest among scientists because it offers the potential of combining the best parts of the characteristic properties of the two entities (e.g., high charge mobility of an inorganic semiconductor and excellent processability of an organic polymer) in a single hybrid. A large number of hybrid materials have been prepared and their chemical and physical properties have been investigated.[1−3] Incorporation of soluble conjugated polymers into the hybrids are expected to endow them with excellent processability and unique materials properties arising from the molecular interactions between the two building blocks, which may find potential applications in photoelectronic devices such as light-emitting diodes (LEDs), photovoltaic cells (PVCs), and field-effect transistors. Exciting results have been obtained along this line of research endeavor. For example, PVCs with high external quantum efficiency (>54%) have been fabricated from the hybrids of a poly(thiophene) (PTh) derivative with a high regioregularity and CdSe nanorods with a large aspect ratio.[1] The devices of the hybrids of poly(phenylenevinylene) (PPV)/ZnO and polyfluorene (PF)/CdSe showed impressive PVC and LED performances.[1]

Polyacetylene is an archetypal π-conjugated polymer and the best-known "synthetic metal", due to the metallic conductivity of its doped form. Its derivatives bearing appropriate substituents (or substituted polyacetylenes) exhibit a variety of novel properties, such as liquid crystallinity, light emission, optical nonlinearity, photoconductivity, and biocompatibility.[4] While the derivatives of PPV, PF, and PTh have been hybridized with various inorganic nanomaterials, the hybridizations of substituted polyacetylenes with inorganic nanomaterials have not been well studied.[5,6] Inorganic nanomaterials and organic polymers are inherently mutually immiscible, and only inhomogeneous mixtures are formed when they are forced to mix, due to the self-aggregation and phase separation of the incompatible components. Many approaches have been developed to tackle this problem.[1−3,5−7] Sulfur atom can strongly coordinate with many metals and Group II−VI semiconductors, and this property has been widely used in the area of study on self-assembling monolayers and other supramolecularly organized structures.[8] Introduction of "free" mercapto groups or their protected forms to side chains or terminals of polymers is an efficient, popular way for preparing organic–inorganic hybrids with desired processability.[1−3,7,9] Polyacetylenes containing thiol groups, however, are still rare species.[6,10,11]

In our previous work, we prepared soluble hybrids of poly(phenylacetylene) (PPA) and CdS nanorods by copolymerization of phenylacetylene with the thiol-functionalized phenylacetylene chemisorbed on the surfaces of the CdS nanorods. The films cast from the solutions of the hybrids were found to exhibit improved processability and enhanced photoconductivity.[6] Our initial plan in that work was to prepare the hybrids by incorporating the CdS nanorods into a thiol-functionalized PPA derivative (PPAS, Chart 1) but the synthesis of the polymer was a challenging job. The mercapto group of the monomer (PAS) deactivated the Mo-, W-, Ta-, and Nb-based "classic" catalysts for acetylene polymerization, with no polymeric products obtained from the attempted polymerizations in the presence of the early transition-metal catalysts. Rh complex $[Rh(cod)Cl]_2$ (cod = 1,5-cyclooctadiene) is known to work as an effective catalyst for the polymerizations of phenylacetylene derivatives bearing polar groups.[4,12] Indeed, the Rh-catalyzed polymerization of PAS proceeded rapidly, but the product was insoluble in common organic solvents. Although we finally obtained the hybrids by first assembling the PAS monomers on the CdS surfaces and then copolymerizing the chemisorbed monomers with phenylacetylene, the approach has drawbacks such as long fabrication route, difficult removal of unreacted monomers, and troublesome determination of the contents of the components by multistep processes.[6]

* Corresponding authors. E-mail: sunjz@zju.edu.cn. (J.Z.S.); Phone: +86-571-8795-3797; Fax: 86-571-8795-3734. E-mail: tangbenz@ust.hk. (B.Z.T.); Phone: +852-2358-7375; Fax: +852-2358-1594.
[†] Zhejiang University.
[‡] The Hong Kong University of Science & Technology.

10.1021/ma702337z CCC: $40.75
Published on Web 04/30/2008

Chart 1

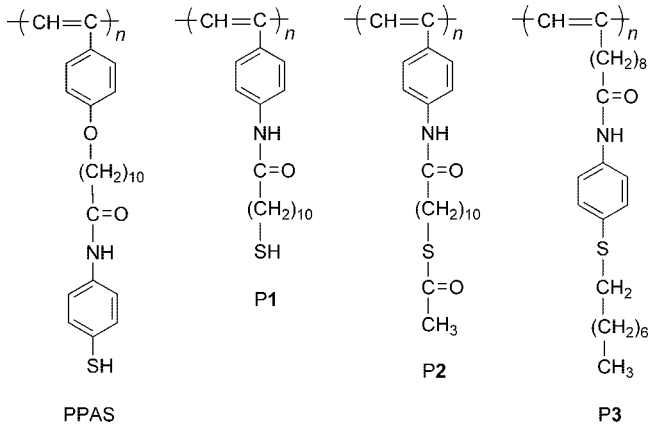

Scheme 1

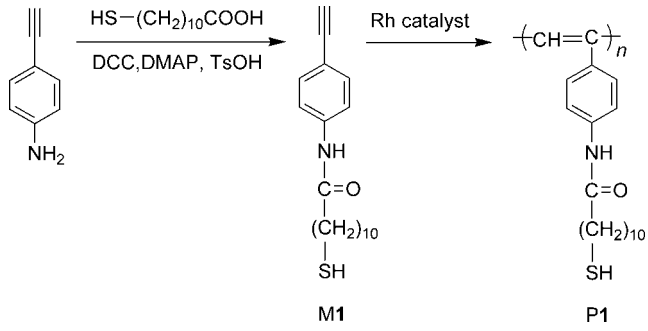

We continued to work in the area. Through modifications of molecular structures, exploration of effective catalysts, and optimizations of reaction conditions, sulfur-containing polyacetylenes (P**1**-P**3**) with good solubility in common solvents were successfully synthesized in this work. The macroscopic processability of the polymers enabled their straightforward hybridizations with ZnO nanoparticles, thanks to the specific interactions of thiol-functionalized polymers with metal-oxide nanoparticles.

Results and Discussion

Polymer Synthesis. In our previous work, the PAS monomer was prepared by a synthetic route as long as six steps, and the resultant polymer was insoluble in common organic solvents.[6] In this work, we designed a one-step route for the preparation of a phenylacetylene derivative bearing a thiol functional group (M**1**, Scheme 1). In M**1**, the mercapto group is linked with the phenylacetylene group via an amide, instead of ether, bond. The mercapto group is located at the end of a flexible decamethylene chain, rather than a rigid phenyl ring. Because of these structural modifications, the monomer was readily prepared in a good yield (68%) under mild reaction conditions.

To polymerize M**1**, we first tried to use $[Rh(cod)Cl]_2$ as catalyst. The polymerization proceeded in the presence of the Rh-based catalyst in a dichloromethane/triethylamine (DCM/TEA) mixture, but the resultant polymer was totally insoluble in common organic solvents (Table 1, no. 1). Similar result was obtained when the polymerization was conducted in tetrahydrofuran (THF)/TEA. Copolymerization did not help; M**1** was copolymerized with phenylacetylene in a wide range of feed ratios but only insoluble products were obtained. With the assumption that the high molecular weight of the product may be responsible for its insolubility, we tried to polymerize M**1** without using TEA, because it is known that TEA speeds up the polymerization reaction and increases the molecular weight of the polymer. No polymer product, however, was obtained in the absence of TEA (Table 1, no. 3). TEA molecule may have coordinated with the metal center and hence protected the catalyst from the toxic effect of the mercapto group.

Table 1. Polymerization of Monomer M1[a]

no.	catalyst	solvent[b]	yield (%)	M_w[c]	M_w/M_n[c]
1	$[Rh(cod)Cl]_2$	DCM/TEA	56.0[d]		
2	$[Rh(cod)Cl]_2$	THF/TEA	60.0[d]		
3	$[Rh(cod)Cl]_2$	DCM	0		
4	Rh^+L	THF	75.0	10 000	1.2
5	Rh^+L	THF	80.0	11 400	1.1

[a] All polymerization reactions were carried out at room temperature under nitrogen for 24 h, except for no. 5, which was conducted for 48 h; $[M]_0$ = 0.2 M, [cat] = 2 mM. Abbreviations: cod = 1,5-cyclooctadiene; Rh^+L = $Rh^+[\eta^6\text{-}C_6H_5(nbd)B^-(C_6H_5)_3]$, nbd = 2,5-norbonadiene; DCM = dichloromethane; TEA = triethylamine; and THF = tetrahydrofuran. [b] In the DCM/TEA or THF/TEA mixture, one drop of TEA was used. [c] Weight-average molecular weight (M_w) and polydispersity index (PDI) determined by gel permeation chromatography (GPC) in THF on the basis of a polystyrene calibration. [d] Insoluble in common organic solvents.

Chain regioregularity of the polymer is another factor that may affect its solubility. $[Rh(cod)Cl]_2$ is such a catalyst that mainly generates regioregular *Z*-rich polymers, especially from the monomers of phenylacetylene derivatives.[12,13] The regularity of the polymer chains facilitates the formation of intra- and intermolecular hydrogen bonds between the amide groups and enhances the interactions between the mercapto groups. These bonding sites serve as "physical cross-linking" points, and consequently the polymers become insoluble gels.

We tried to use a zwitterionic rhodium complex of $Rh^+[\eta^6\text{-}C_6H_5(nbd)B^-(C_6H_5)_3]$ as catalyst. To our delight, the catalyst worked well to produce soluble polymers in high yields (75–80%, Table 1, nos. 4 and 5). The good solubility of polymers enabled their molecular weight measurements. The polymer obtained after 24 h polymerization has a molecular weight of 10 000. Extension of the reaction time to 48 h exerted little effect on the yield and molecular weight of the polymer as well as its polydispersity index. These results indicate that the polymerization reactions catalyzed by the zwitterionic complex have proceeded in moderate rates.

By use of the zwitterionic complex as catalyst, the PAS monomer was also polymerized. The resultant polymer was, however, only partially soluble. The soluble fraction became insoluble after stored under ambient conditions for a few weeks. This storage-induced insolubility was also observed in P**1**. These results suggest that the rigidity of the phenyl ring linking with the mercapto group has exerted little effect on the solubility and that the free mercapto groups have played an important role in determining the solubility of the polymers. The mercapto groups are chemically reactive. The interactions between the mercapto groups in different polymer chains, for example, may result in the formation of dithiols, accounting for the storage instability of the polymers. We thus designed a new monomer (M**2**) by replacing the mercapto hydrogen with an acetyl group.

Following the design principle elaborated above, the new acetylene monomer with its mercapto group capped by an acetyl group (M**2**) was prepared by the synthetic route shown in Scheme 2. When M**2** was polymerized in DCM/TEA, only red, insoluble products were formed (Table 2, nos. 1 and 2). In the absence of TEA, no polymerization reaction occurred. Delightfully, however, when the solvent was changed from DCM to THF, brown, soluble product with a moderate molecular weight of 8200 was obtained in an acceptable yield (53%; Table 2, no.4). Copolymerizing M**2** with phenylacetylene gave soluble polymeric products with high molecular weights ($M_w \geq 40\,000$) in excellent yields (>86%). The products maintained solubility even after being stored for a whole year. These results verified our molecular design rationale and confirmed our suspect that

Scheme 2

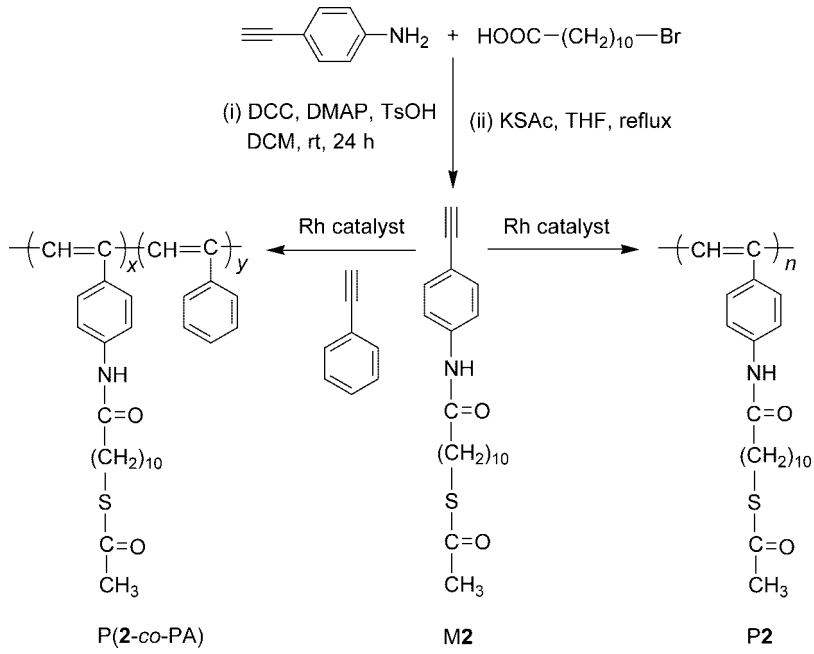

Table 2. Homopolymerization of Monomer M2 and its Copolymerization with PA[a]

no.	[2]:PA[b]	solvent[c]	yield (%)	M_w[d]	M_w/M_n[d]
		homopolymerization			
1	1:0	DCM/TEA	66.5[e]		
2	1:0	DCM/TEA	57.3[e]		
3	1:0	DCM	0		
4	1:0	THF/TEA	53.0	8200	1.5
		copolymerization			
5	1:1	DCM/TEA	95.2	101 400	2.2
6	1:3	DCM/TEA	86.4	96 200	2.1
7	1:6	DCM/TEA	97.3	122 500	2.2
8	1:9	DCM/TEA	96.3	40 000	1.9

[a] All polymerization reactions were carried out with $[Rh(cod)Cl]_2$ at room temperature under nitrogen for 24 h, except for no. 2, which was conducted for 4 h; $[M]_0 = 0.2$ M, [cat] = 2 mM. [b] Molar ratio. [c] In the DCM/TEA or THF/TEA mixture, one drop of TEA was used. [d] Weight-average molecular weight (M_w) and polydispersity index (PDI) determined by gel permeation chromatography (GPC) in THF on the basis of a polystyrene calibration. [e] Insoluble in common organic solvents.

physical cross-linking between the free mercapto groups was responsible for poor solubility of PPAS and P**1**.

We further designed a new thioacetylene monomer with a different molecular structure (M**3**), which was prepared according to the synthetic route shown in Scheme 3. The monomer was a 1-alkyne, rather than phenylacetylene, derivative with its mercapto group capped by a long alkyl chain, instead of an acetyl group. We initially worried that it might not be easy to transform M**3** to its polymer, because it is known that 1-alkynes, especially those containing polar groups, are difficult to polymerize.[4,10,14] Indeed, polymerization of M**3** by $[Rh(cod)Cl]_2$ gave a polymeric product in a low yield of 20% (Table 3, no. 1). Happily, however, $Rh^+[\eta^6\text{-}C_6H_5(nbd)B^-(C_6H_5)_3]$ was found to perform well as a catalyst. When M**3** was polymerized in DCM in the presence of the zwitterionic complex, a polymer with a molecular weight of 11 400 was obtained in 53% yield. When the solvent was changed to THF, both the polymer yield (83%) and the molecular weight (15 800) increased (Table 3, no. 3). Evidently, $Rh^+[\eta^6\text{-}C_6H_5(nbd)B^-(C_6H_5)_3]$ is an effective catalyst for the polymerization of the thioalkyne monomer. In comparison to DCM, THF is a better solvent, probably because the zwitterionic complex likes the hydrophilic, polar solvent. The resultant polymer (P**3**) can be dissolved in common organic solvents, including DCM, THF, chloroform, *N,N*-dimethylmethanamide (DMF), and toluene.

Structural Characterization. The polymeric products were characterized by spectroscopic methods, from which satisfactory analysis data were obtained (see Experimental section for details). The ^{1}H NMR spectrum of P**1** is shown in Figure 1 along with that of M**1** (for comparison). The spectrum of M**1** shows a peak at δ 4.0, due to the resonance of its acetylene proton. This peak cannot be found in the spectrum of P**1**. Instead, a new peak associated with the resonance of olefinic proton is observed at $\delta \sim 6.3$. This indicates that the acetylenic triple bond in M**1** has been transformed to olefinic double bond in P**1** by the polymerization reaction. The resonance peaks of phenyl protons in M**1** appear at δ 7.6 and 7.4. After polymerization, the two peaks are broadened and upfield shifted to δ 7.5 and 7.3, respectively, because of the conjugation of the phenyl ring with the polyene backbone.

Figure 2 shows the ^{13}C NMR spectra of P**1** and M**1**. Whereas the acetylenic carbon atom linked with the phenyl ring of M**1** resonates at $\delta \sim 84.6$, this peak is completely absent in the spectrum of P**1**. The resonance peak of the terminal carbon atom (H*C*≡) cannot be seen in the spectrum of M**1**, probably due to its overlap with the peaks of the solvent. Two new resonance peaks are observed at δ 138.0 and 116.1, due to the resonance of the polyene carbons of P**1**. This further confirms that the polymerization has been realized through the transformation of the triple bonds of the monomers to the double bonds of the polymer. Since the phenyl ring is conjugated with the polyene backbone after polymerization, the resonance of the phenyl carbon directly linked with the double bond is downfield shifted from δ 117.4 to ~132.0, as observed in our previous studies.[15]

The ^{1}H NMR spectra of P**2** and M**2** are shown in Figure 3. The peak at δ 3.0 in the spectrum of M**2** is assigned to the resonance of its acetylene proton. The disappearance of this peak in the spectrum of P**2** indicates that the monomer has been consumed by the polymerization reaction. Intriguingly, the peaks corresponding to the resonances of the protons of the polyene backbone, phenyl ring, and amide group are hardly recognized in the spectrum of P**2**, although the expected peaks are all discernible in the magnified spectrum (Figure 3B, inset). In sharp contrast, the resonance peaks of the protons of the alkyl pendant can be clearly seen in the upfield region of the spectrum. Similar

Scheme 3

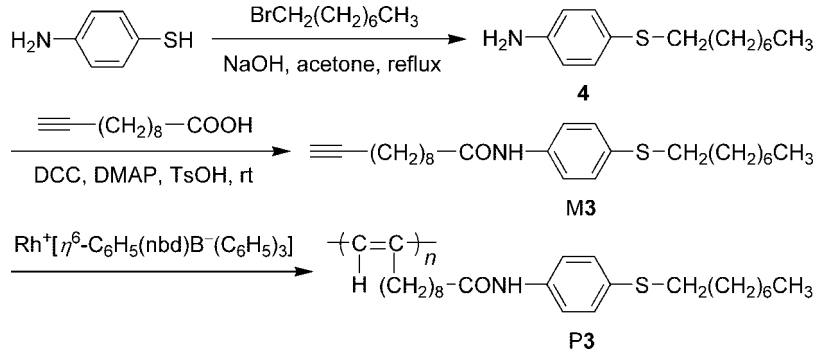

Table 3. Polymerization of Monomer M3[a]

no.	catalyst	solvent[b]	yield (%)	M_w[c]	M_w/M_n
1	$[Rh(cod)Cl]_2$	DCM/TEA	20.0	6 700	1.2
2	Rh^+L	DCM	53.3	11 400	1.1
3	Rh^+L	THF	83.0	15 800	1.1

[a] All polymerization reactions were carried out at room temperature under nitrogen for 24 h. [b] In the DCM/TEA mixture, one drop of TEA was used. [c] Weight-average molecular weight (M_w) and polydispersity index (PDI) determined by gel permeation chromatography (GPC) in THF on the basis of a polystyrene calibration.

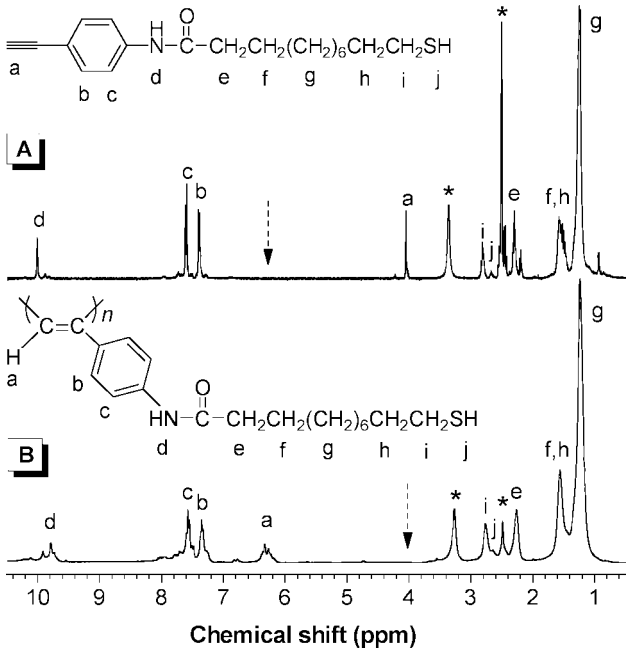

Figure 1. ^1H NMR spectra of (A) monomer M**1** and (B) its polymer P**1** in dimethylsulfoxide (DMSO)-d_6. The solvent and water peaks are marked with asterisks.

spectra are obtained in benzene-d_6 and DMSO-d_6 at room temperature and elevated temperature (Figure 4). These spectral data indicate that the motions of the polyene backbone, phenyl rings, and amide group are highly restricted in the polymer solutions.

The ^{13}C NMR spectra of P**2** and M**2** are shown in Figure 5. The peak at δ 83.3 associated with the resonance of the acetylenic carbon atom linked to the phenyl ring is completely absent in the spectrum of P**2**. Here, again, the peaks of the polyene backbone and phenyl ring are not observed but those of the flexible alkyl tails are clearly seen. All the spectral data of P**2** shown in Figures 3, 4, and 5 suggest that some microstructures are formed in its solutions, which restrict the motions of the polyene backbone and phenyl ring.

In our previous studies, we found that some side-chain liquid crystalline (LC) polyacetylenes self-organized into unique nanostructures such as nanorods, nanoparticles, and nanosheets due to microphase separation.[4,16] In the LC polymers, their side chains containing aromatic mesogens and alkyl tails spontaneously assembled into molecular cylinders, and the hard cores restricted the motions of the aromatic mesogens, resulting in the absence of the related proton resonance signals in their NMR spectra. Similar self-organization behavior was observed in side-chain polyamphiphiles.[17] For example, the hydrophobic part of the polymer forms microdomain that is surrounded by a shell of its hydrophilic part in an aqueous solution, yielding a micellar microstructure. The hydrophobic part buried inside the micelle thus becomes NMR-silent and cannot be detected by the spectrometer.

In this regard, P**2** may have also formed some microstructures via self-organization of its rigid PPA skeleton and flexible alkyl

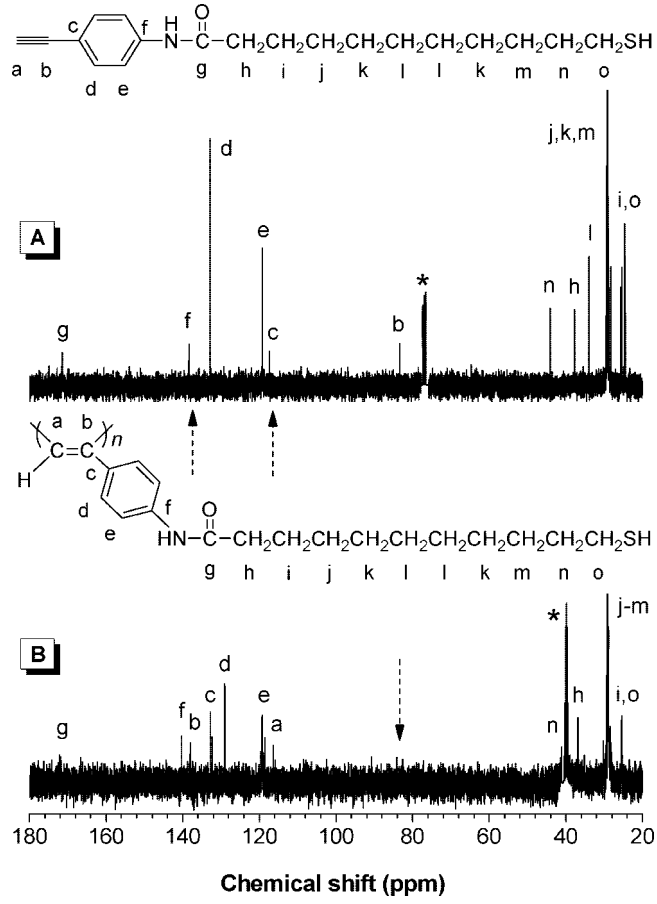

Figure 2. ^{13}C NMR spectra of (A) monomer M**1** in chloroform-d and (B) its polymer P**1** in DMSO-d_6. The solvent peaks are marked with asterisks.

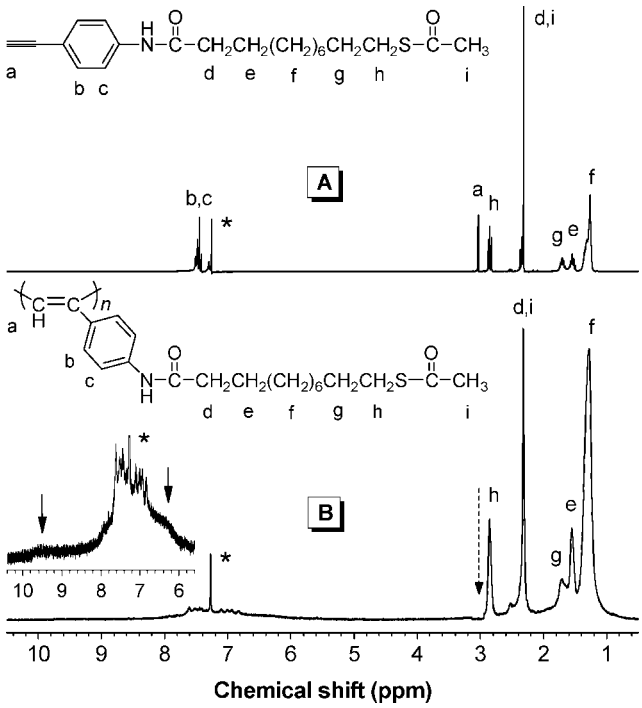

Figure 3. ^{1}H NMR spectra of (A) monomer M**2** and (B) its polymer P**2** in chloroform-*d*. The solvent peaks are marked with asterisks.

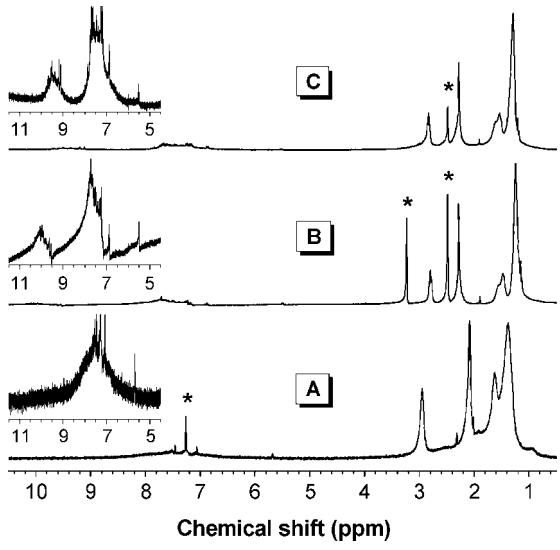

Figure 4. ^{1}H NMR spectra of P**2** in (A) benzene-d_6, (B) DMSO-d_6 at room temperature (~23 °C), and (C) DMSO-d_6 at 120 °C. The solvent and water peaks are marked with asterisks.

pendant. Indeed, nanostructures such as nanoparticles, nanosheets, and nanotubes are observed by transmission electron microscope (TEM) measurements of the samples prepared by dropping dilute THF solutions of P**2** onto copper grids (Figure 6). The self-organization of the P**2** chains into nanoparticles is also confirmed by the scanning electron microscope (SEM) measurement of the interface layer formed by adding hexane to a DCM solution of the polymer.

Figure 7 shows the ^{1}H NMR spectra of P**3** and M**3**. The monomer exhibits a single peak at δ 1.9, which can be ascribed to its acetylene proton. This peak is totally absent in the NMR spectrum of the polymer, proving that no monomer is left in the polymer product. This point is further confirmed by the ^{13}C NMR spectral analysis (Figure 8). The peaks at δ 84.9 and 68.3 for the acetylenic carbon atoms of M**3** are not found in the spectrum of P**3**. New resonance peaks appear at δ 136.4 and

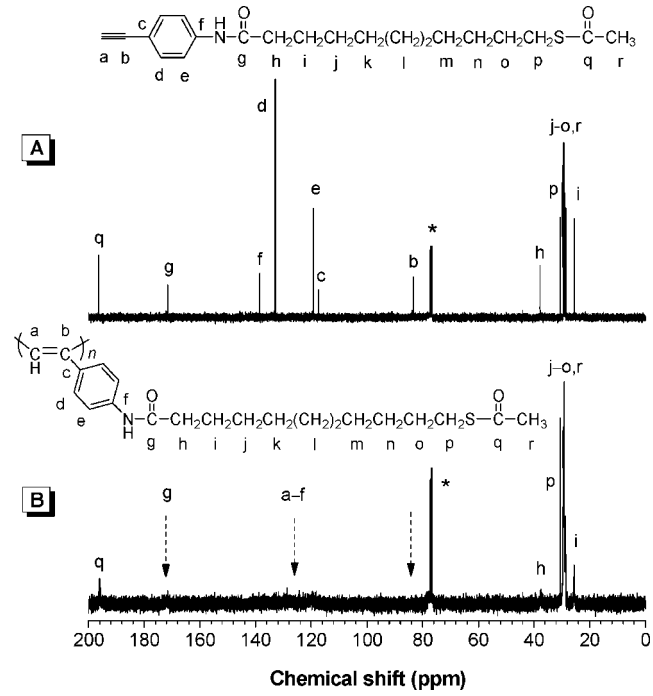

Figure 5. ^{13}C NMR spectra of (A) monomer M**2** and (B) its polymer P**2** in chloroform-*d*. The solvent peaks are marked with asterisks.

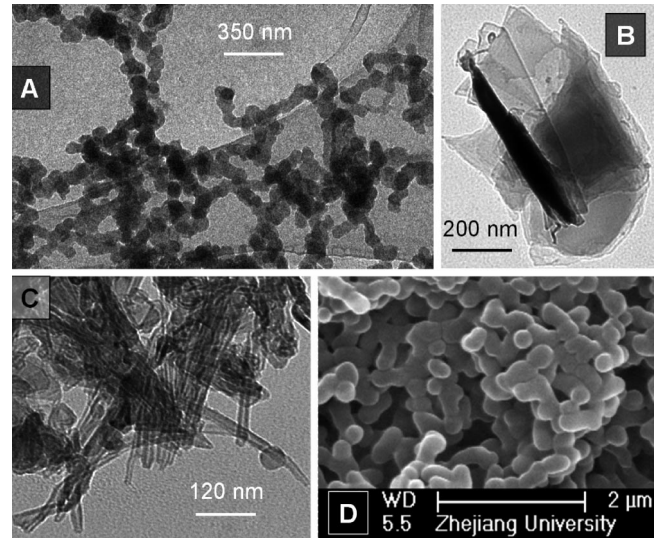

Figure 6. TEM images of (A) nanoparticles, (B) nanosheets, and (C) nanotubes of P**2** and (D) SEM image of its nanoparticles.

119.5, which are assignable to the polyene carbon atoms of P**3**. The propargylic carbon of M**3** is transformed to the allylic one of P**3**, and the δ value is accordingly downfield shifted from 18.6 to 31.8.

Polyacetylene/ZnO Hybridization. The successful syntheses of the sulfur-containing polyacetylenes with microscopic processability offer us a unique opportunity to prepare nanohybrids of polyacetylenes with inorganic semiconductor nanostructures, which may bring the advantages of the two components into full play. Polyacetylenes are p-type semiconductors,[4] while ZnO is an n-type semiconductor. We hybridized the poly(thioacetylene)s with ZnO nanoparticles in anticipation that the resultant hybrids may exhibit useful optoelectronic properties.

The hybrids were prepared by simply mixing and stirring the polymers and ZnO nanoparticles in a solvent such as THF. Taking P**2** as an example, the polymer can be dissolved in THF in a concentration of up to ~6 mg/mL, giving a clear, brownish-

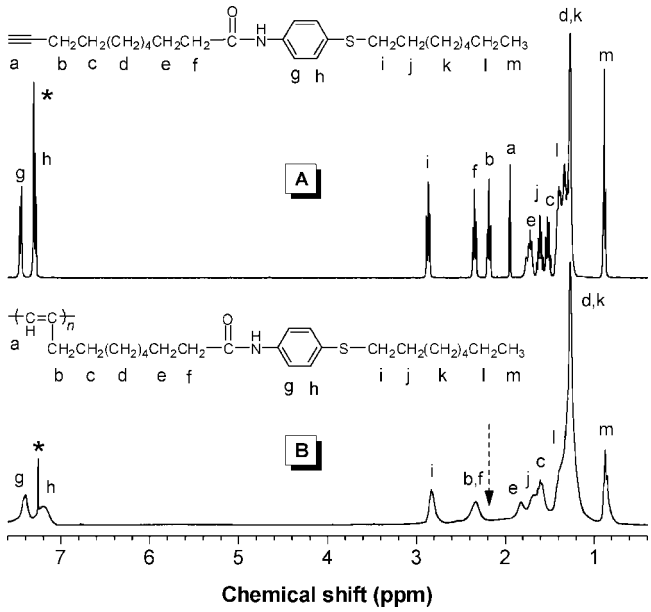

Figure 7. ^{1}H NMR spectra of (A) monomer M**3** and (B) its polymer P**3** in chloroform-*d*. The solvent peaks are marked with asterisks.

yellow solution (Figure 9). While the ZnO nanoparticles are not soluble in THF, the P**2**/ZnO hybrids can disperse well in THF and other common organic solvents, such as DCM, DMF, DMSO, and toluene. The hybrid suspensions are stable, with no obvious precipitate formed after standing for several days.

The formation of homogeneous suspension results from the attractive interactions between the sulfur functional group in P**2** and the ZnO nanoparticles.[8] Photoluminescence (PL) spectra of the nanohybrids offer valuable information about the interactions between the two components. As can be seen from Figure 10, ZnO nanoparticles shows a broad peak at 500 nm, which is referred to as deep-level emission band and is attributed to the oxygen vacancies in ZnO.[18] This peak is changed to a shoulder in the spectrum of the P**2**/ZnO hybrid suggestive of the existence of some special photophysical processes in the hybrid. One possible process is the energy transfer from ZnO to P**2**, which is, however, unreasonable because the emission band of ZnO completely mismatches with the absorption band of P**2** (cf. Supporting Information, Figure S2).

Another possible process is the charge transfer between P**2** and ZnO. Charge transfer is usually associated with photoinduced electron transfer from a conjugated polymer (donor) to a semiconductor nanostructure (acceptor), which leads to PL quenching of the conjugated polymer. In our case, however, what has been quenched is the PL from the ZnO nanoparticles. The charge transfer process can thus be excluded. A rational explanation is that the oxygen vacancies have been effectively filled by the sulfur functional groups of P**2**, which have destroyed the deep-level emission centers of the ZnO nanoparticles. Consequently, the emission dominated by oxygen vacancies is quenched.

The PL spectrum of the hybrid is broader and its emission peak at ~400 nm is higher, in comparison with those of P**2**. The spectral broadening may be caused by the strong interactions between P**2** and ZnO, which may induce the polymer chain to take a more conjugated conformation. This is, however, not the case, because no obvious changes in the absorption spectrum of P**2** have been observed. The inorganic component thus must have played a key role. Actually, besides the deep-level emission, ZnO exhibits a near-band-edge (NBE) band,[18] which is assigned to the intrinsic emission of ZnO. The NBE band generally extends from 360 to 420 nm, superposing with the emission of P**2**. In other words, when the oxygen vacancies of ZnO are filled by the sulfur atoms of P**2**, the deep-level emission of ZnO is suppressed and its NBE emission becomes dominative. As a result, the intensity of the emission at ~400 nm is increased, and its band shape is broadened.

To show the attractive interactions of the poly(thioacetylene)s with ZnO nanoparticles, the following experiment was carried out. The thin films of P**1**−P**3** and PPA were cast onto quartz plates from their solutions (3 mg/mL) in DCM. After drying, the films were dipped perpendicularly into a suspension of ZnO nanoparticles in ethanol (0.5 mg/mL) for 1 h and then taken out and rinsed with ethanol several times. The surface morphologies of the thin films were measured by atomic force microscope (AFM) in a tapping mode. A typical AFM image of the as-prepared film of P**2** is shown in Figure 11A (10 × 10 μm^2). The image reveals that the film surface is a flat plane dotted with sporadic pinholes and dots. The maximum fall from the acme of the dot to the bottom of the pit is merely ~28 nm, indicating that the surface of the film is quite smooth.

In sharp contrast, after dipping the P**2** film into the suspension of the ZnO nanoparticles, the surface morphology changed greatly, with particles 100–200 nm in size spread over the film surface (Figure 11B). The maximal fall from the top of the particle to the bottom of the furrow is ~235 nm, much larger than that in Figure 11A. The particles on the film surface are confirmed to be ZnO nanoparticles (see Supporting Information). On the other hand, the AFM image of the PPA film is featured by a smooth plane with fluctuations as small as ~15 nm. After dipping into the ZnO nanoparticle suspension, the film changes little in its morphology, with only tiny dots sparsely left on the surface. The AFM image shown in Figure 11B thus verifies that the ZnO nanoparticles have been chemisorbed onto the surface of P**2** film. The driving force is the attractive interactions between the sulfur atoms of the polymer and the Zn cations of the nanoparticles.

Thin films of the P**2**/ZnO hybrids were prepared by casting their THF solutions. As can be seen from the example of SEM image shown in Figure 12A, the nanoparticles are well dispersedly in the film with a smooth surface. On the other hand, in the film prepared from the PPA/ZnO blend, the nanoparticles agglomerate into large aggregates and the surface is uneven. According to the principle of SEM, the particle-like objects with high contrast are ZnO nanoparticles. This is further confirmed by the energy dispersive X-ray (EDX) analysis, which proves the existences of zinc element in the agglomerate and sulfur element in the film.

Concluding Remarks. In summary, we have synthesized three new sulfur-containing polyacetylenes (P**1**−P**3**) in this work. We have changed the spacer between the mercapto and phenylacetylene groups (in M**1**), capped the free thiol by an acetyl group (in M**2**), and used a flexible 1-alkyne skeleton along with a long alkyl capper (in M**3**). We have employed the zwitterionic complex $Rh^+[\eta^6\text{-}C_6H_5(nbd)B^-(C_6H_5)_3]$ as catalyst. Our efforts in the molecular structure design and reaction condition optimization have enabled us to successfully tackle the toxic effect of the thiol group and the poor solubility of the polyacetylenes.

Films are formed when the solutions of P**1**−P**3** are cast onto quartz, glass, and metal substrates. ZnO nanoparticles are chemisorbed onto the surfaces of the polymer films via attractive interactions between thiol groups and zinc cations. This provides a simple method for selectively attaching appropriate inorganic nanoparticles onto patterned surfaces of sulfur-containing polymers. Stable suspensions of polyacetylene/ZnO hybrids are prepared by simply mixing the two components in common organic solvents. These results demonstrate that the soluble and tractable sulfur-containing polyacetylenes are useful functional

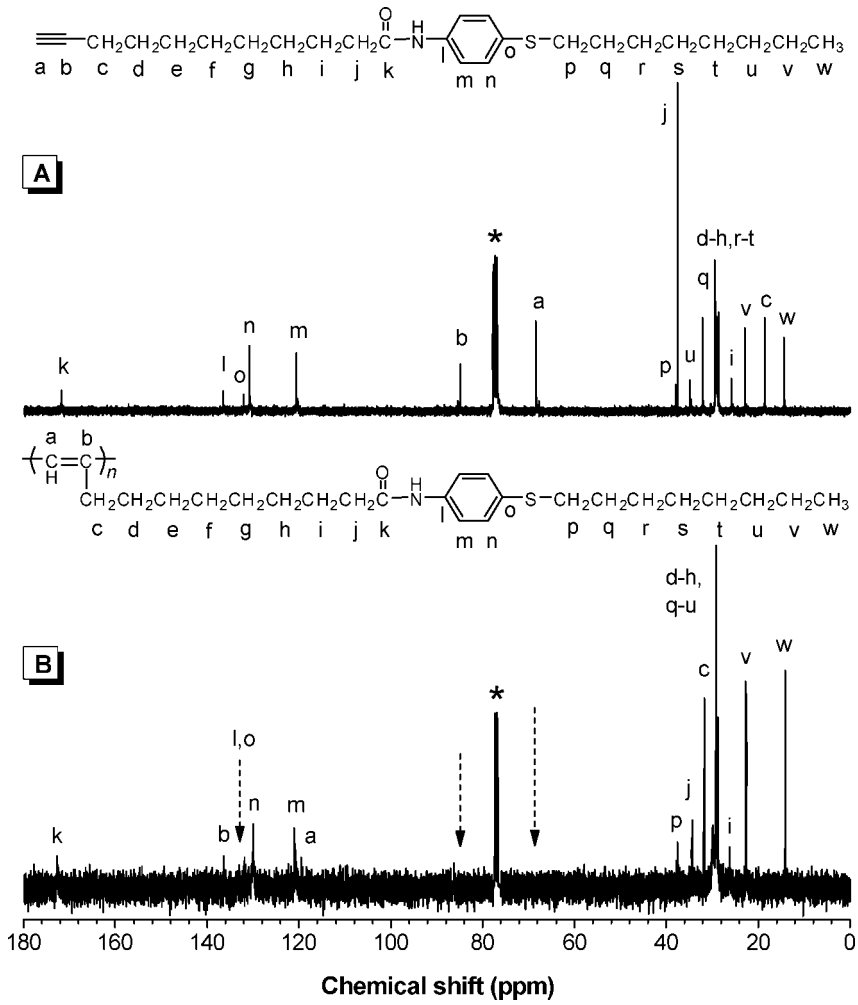

Figure 8. ^{13}C NMR spectra of (A) M**3** and (B) its polymer P**3** in chloroform-*d*. The solvent peaks are marked with asterisks.

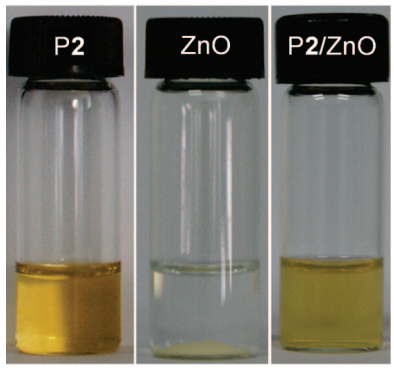

Figure 9. Photographs of polymer P**2**, ZnO nanoparticles, and P**2**/ZnO hybrids in THF.

materials for the fabrication of nanohybrids with inorganic nanostructures.

Experimental Section

Materials. THF was distilled under normal pressure from sodium benzophenone ketyl under argon immediately prior to use. DCM was dried over 4 Å molecular sieves and distilled over calcium hydride. TEA was distilled and dried over KOH. Acetone was dried over 4 Å molecular sieves prior to use. ZnO nanoparticles with an average size of ~100 nm were prepared in our laboratories by solvothermal process. 11-Bromoundecanoic acid, 4-ethynylaniline (both from TCI), 4-(dimethylamino)pyridine (DMAP), 11-mercaptoundecanoic acid (both Aldrich), 4-aminothiophenol, phenylacetylene, potassium thioacetate (all from Acros), 10-undecynoic acid (ABCR), *N,N'*-dicyclohexylcarbodiimide (DCC), *p*-toluenesulfonic acid monohydrate (TsOH), sodium hydroxide, and 1-bromooctane (all from SCR) were all purchased in analytical grades and used as

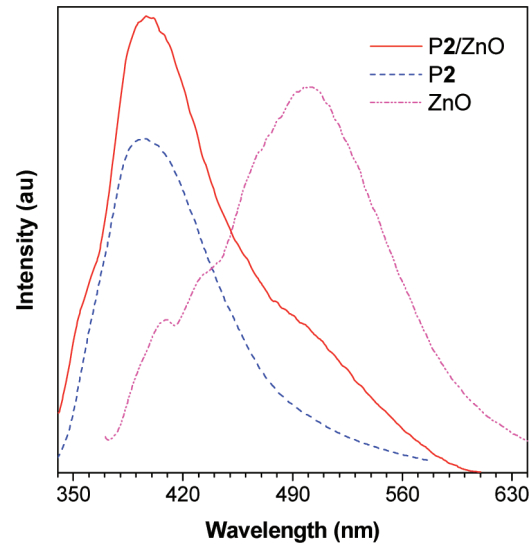

Figure 10. Emission spectra of solution of P**2** and suspensions of ZnO nanoparticles and P**2**/ZnO hybrid in THF. Concentration of P**2** was kept at 1×10^{-4} M in the solution and suspension, while that of the ZnO nanoparticles was determined by its content in the hybrid. Excitation wavelength: 320 nm (for P**2** and P**2**/ZnO hybrid) and 350 nm (for ZnO nanoparticles).

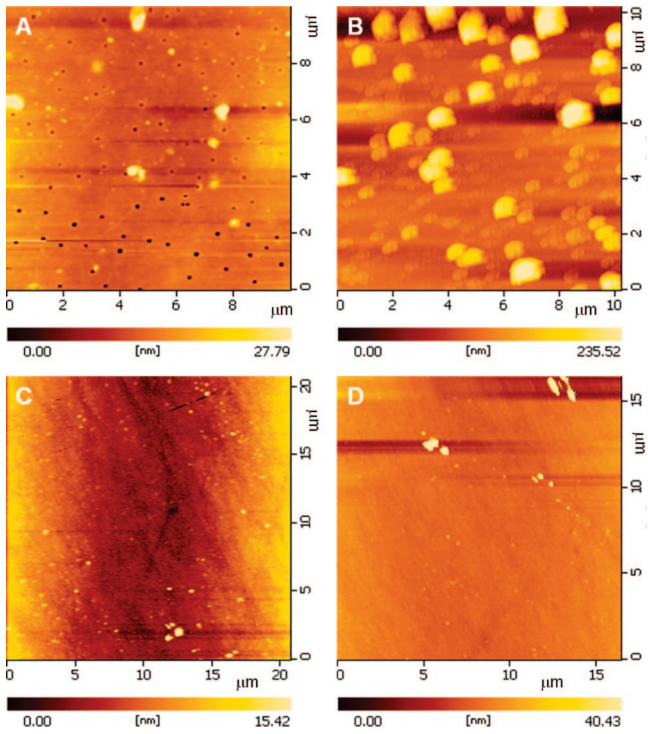

Figure 11. AFM images of a P**2** film cast on a quartz plate (A) before and (B) after dipping into a suspension of ZnO nanoparticles in ethanol (0.5 mg/mL). The images for a PPA film (C) before and (D) after dipping into the ZnO suspension are shown for comparison.

received without further purifications. Organorhodium complexes of $[Rh(cod)Cl_2]_2$ and $Rh^+[\eta^6\text{-}C_6H_5(nbd)B^-(C_6H_5)_3]$ were prepared according to published procedures.[19,20]

Instrumentation. The ^1H and ^{13}C NMR spectra were measured on a Mercury plus NMR 300 MHz nuclear resonance spectrometer using tetramethylsilane (TMS, $\delta = 0$ ppm) as the internal standard. The IR spectra were measured on a Bruker VECTOR 22 spectrometer. The UV–vis absorption spectra were recorded on a Varian CARY 100 Bio spectrophotometer. The PL spectra were measured on a Hitachi 4500 fluorescence spectrophotometer. The average molecular weights (M_w and M_n) and PDIs of the polymers were estimated by a Waters Associated GPC system in THF. A set of monodisperse polystyrene standards covering a molecular weight range of 10^3-10^7 was used for the molecular weight calibration. TGA was carried out on a Pyris 6 thermogravimetric analyzer (Perkin-Elmer), in which a sample of ~3 mg was heated up to 700 °C at a rate of 10 °C/min under a flow of nitrogen stream.

The SEM images were taken on a JSM-5510 microscope coupled with an EDX analyzer, and the TEM images were obtained on a JEM-200CX microscope. The X-ray diffraction (XRD) patterns (scanning range 10–60°) were measured on a D/max rA diffractometer equipped with a graphite monochromatized Cu Kα radiation ($\lambda = 1.5405$ Å) operating at 40 mA and 40 kV. The AFM images were recorded on a SPI 3800N microscope in a tapping mode.

Monomer Synthesis. Monomers M**1**−M**3** were prepared according to the synthetic routes shown in Schemes 1–3. Detailed experimental procedures are given below.

*N-(4-Ethynylphenyl)-11-mercaptoundecanamide (M**1**).* Into a 250 mL round-bottom flask were added 900 mg (7.63 mmol) of 4-ethynylaniline, 2 g (9.16 mmol) of 11-mercaptoundecanoic acid, 2.36 g (11.45 mmol) of DCC, 186 mg (1.53 mmol) of DMAP, and 290 mg (1.53 mmol) of TsOH. The contents were dissolved in 150 mL of DCM and then stirred at room temperature for 24 h under nitrogen. After filtering the urea salts formed during the reaction, the solid was washed with diethyl ether and the filtrate was concentrated using a rotary evaporator. The residue was purified on a silica gel column using a mixture of chloroform/hexane (1:1, v/v) as eluent. Removal of the solvents gave 1.66 g of a light yellow solid of M**1** (yield: 68.4%). ^1H NMR (300 MHz, DMSO-d_6, δ): 10.0 (s, H, N*H*), 7.6 (d, 2H, aromatic protons *ortho* to NH), 7.4 (d, 2H, aromatic protons *meta* to NH), 4.0 (s, H, *H*C≡C), 2.8 (t, 2H, CH_2S), 2.3 (t, 2H, COCH_2), 2.2 (m, H, S*H*), 1.4–1.6 (m, 4H, $COCH_2CH_2$ and $HSCH_2CH_2$), 1.0–1.4 [m, 12H, $(CH_2)_6$]. ^{13}C NMR (75 MHz, $CDCl_3$, δ): 171.4 (*C* = O), 138.4 (aromatic carbon *para* to C≡C), 132.9 (aromatic carbons *ortho* to C≡C), 119.2 (aromatic carbons *meta* to C≡C), 117.3 (aromatic carbon attached to C≡C), 84.6 (Ph*C*≡), 44.1 (CH_2CH_2SH), 37.7 (CO*C*H_2), 33.9 [$COCH_2$-$CH_2CH_2CH_2(CH_2)_2$], 29.6, 29.1, 28.7 [$COCH_2CH_2(CH_2)_2$ and $(CH_2)_2CH_2CH_2SH$], 25.4 ($COCH_2CH_2$), 24.6 (CH_2SH). Anal. Calcd for $C_{19}H_{27}NOS$ (317.49): C, 71.88; H, 8.57; N, 4.41. Found: C, 71.69; H, 8.94; N, 4.30. MS (*m*/*z*): 316.1 [$(M-1)^+$].

*S-10-(4-Ethynylphenylcarbamoyl)decyl Ethanethioate (M**2**).* This monomer was synthesized in two steps. 11-Bromo-*N*-(4-ethynylphenyl)undecanamide was first prepared by a procedure similar to that used for the preparation of M**1**. A white solid was obtained in 87.6% yield. Then 1.2 g (3.3 mmol) of the product, 1.14 g (10 mmol) of potassium ethanethioate, and 100 mL of THF were added into a 250 mL round-bottom flask. The mixture was refluxed overnight under nitrogen. The solvent in the reaction mixture was evaporated and the crude product was extracted with DCM. The combined organic layers were dried over Na_2SO_4 and concentrated. The residue was purified by a silica gel column using chloroform as eluent. A yellowish solid of M**2** was obtained in 100% yield. ^1H NMR (300 MHz, $CDCl_3$, δ): 7.4–7.6 (m, 4H, aromatic protons), 3.0 (s, H, *H*C≡C), 2.8 (t, 2H, CH_2S), 2.2–2.4 (m, 5H, COCH_2 and CH_3), 1.7 (m, 2H, CH_2CH_2S), 1.5 (m, 2H, $COCH_2CH_2$), 1.2–1.4 [m, 12H, $(CH_2)_6$]. ^{13}C NMR (75 MHz, $CDCl_3$, δ): 196.2 (S*C*O), 171.6 (NH*C*O), 138.5 (aromatic carbon *para* to C≡C), 132.8 (aromatic carbons *ortho* to C≡C), 119.3 (aromatic carbons *meta* to C≡C), 117.4 (aromatic carbon attached to C≡C), 83.3 (Ph*C*≡), 37.8 (CO*C*H_2), 30.7 (CH_2S), 29.5, 29.2, 29.0, 28.6 [$COCH_2CH_2(CH_2)_7$], 25.4 (*C*H_3). Anal. Calcd for $C_{21}H_{29}NO_2S$ (359.53): C, 70.15; H, 8.13; N, 3.90. Found: C, 69.89; H, 8.17; N, 4.11. MS (*m*/*z*): 316.1 [$(M-CH_3CO)^+$].

*4-(Octylthio)aniline (**4**).* To a 150-mL acetone solution containing sodium hydroxide (0.76 g, 19.02 mmol) and 4-aminothiophenol (2 g, 15.85 mmol), 3.67 g (19.02 mmol) of 1-bromooctane was added. The mixture was refluxed for 12 h. After evaporation of acetone from the solution, the product was purified by silica gel column chromatography using a mixture of chloroform/hexane (1:1, v/v) as eluent. A white solid of **4** was obtained in 91.6% yield. ^1H NMR (300 MHz, $CDCl_3$, δ): 7.2 (d, 2H, aromatic protons *meta* to NH_2), 6.6 (d, 2H, aromatic protons *ortho* to NH_2), 3.6 (s, 2H, NH_2), 2.7 (t, 2H, SCH_2), 1.6 (m, 2H, SCH_2CH_2), 1.1–1.4 [m, 10H, SCH_2-$CH_2(CH_2)_5$], 0.9 (m, 3H, CH_3).

*N-[4-(Octylthio)phenyl]-10-undecynamide (M**3**).* This monomer was synthesized from **4** and 10-undecynoic acid by a procedure similar to that used for the preparation of M**1**. A white solid was obtained in 88.0% yield. ^1H NMR (300 MHz, $CDCl_3$, δ): 7.5 (d, 2H, aromatic protons *ortho* to NH), 7.3 (d, 2H, aromatic protons *meta* to NH), 2.8 (m, 2H, PhSCH_2), 2.3 (t, 2H, CH_2CO), 2.2 (t, 2H, ≡CCH_2), 1.9 (t, H, *H*C≡C), 1.7 (m, 2H, CH_2CH_2CO), 1.6 (m, 2H, SCH_2CH_2), 1.5 (m, 2H, ≡CCH_2CH_2), 1.1–1.4 [m, 18H, ≡$CCH_2CH_2(CH_2)_4$ and $(CH_2)_5CH_3$], 0.9 (m, 3H, CH_3). ^{13}C NMR (75 MHz, $CDCl_3$, δ): 171.8 (*C*ONH), 136.4 (aromatic carbon attached to NH), 131.9 (aromatic carbon *para* to NH), 130.8 (aromatic carbons *meta* to NH), 120.6 (aromatic carbons *ortho* to NH), 84.9 (HC≡*C*), 68.3 (*H*C≡C), 38.0 (SCH_2), 37.6 (CH_2CO), 34.8 ($CH_2CH_2CH_3$), 32.0 (SCH_2CH_2), 29.5, 29.4, 29.2 29.0, 28.8, 28.6 [≡$CCH_2(CH_2)_5$], 25.8 (CH_2CH_2CO), 22.8 (CH_2CH_3), 18.6 (≡CCH_2), 14.3 (*C*H_3). Anal. Calcd for $C_{25}H_{39}NOS$ (401.65): C, 74.76; H, 9.79; N, 3.49. Found: C, 74.80; H, 9.85; N, 3.75. MS (*m*/*z*): 400.3 [$(M-1)^+$].

Polymerization Reactions. All the polymerization reactions and manipulations were carried out under dry nitrogen using Schlenk techniques in a vacuum-line system, except for the purification of the polymers, which was done in an open atmosphere. The synthetic routes to the polymers are shown in Schemes 1–3. Typical

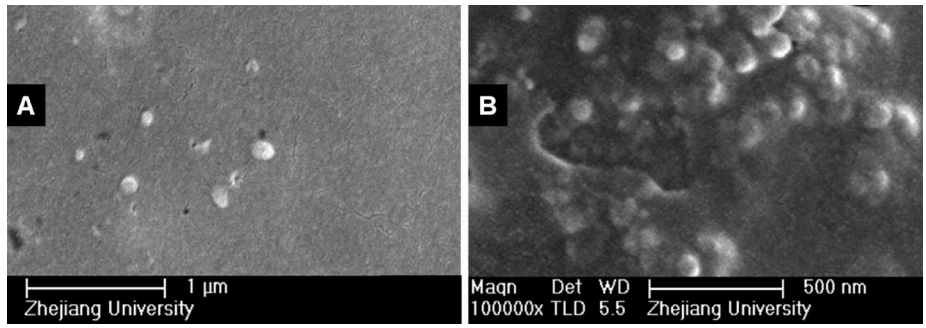

Figure 12. SEM images of thin films cast from THF solutions of (A) P**2**/ZnO hybrid and (B) PPA/ZnO blend.

experimental procedures for the polymerization of M**1** are given below as an example.

Into a baked 20 mL Schlenk tube with a sidearm was added 160 mg (0.5 mmol) of M**1**. The tube was evacuated under vacuum and flushed with dry nitrogen three times through the sidearm. THF (1.5 mL) was then injected. The catalyst solution was prepared in another tube by dissolving 2.5 mg of $Rh^+[\eta^6\text{-}C_6H_5(nbd)B^-(C_6H_5)_3]$ in 1 mL of THF, which was transferred to the monomer solution using a hypodermic syringe. The reaction mixture was stirred at 30 °C under nitrogen for 24 h. The mixture was then diluted with 6 mL of THF and added dropwise to 500 mL methanol through a cotton filter under stirring. The precipitate was allowed to stand for 24 h and then filtered with a Gooch crucible. The polymer was washed with methanol for five times and dried in a vacuum oven at 40 °C to a constant weight.

*Characterization Data of Polymers. P***1**. This polymer was obtained as a yellow powdery solid in 80.0% yield (Table 1, no. 4). M_w = 11 400; M_w/M_n = 1.1. ^{1}H NMR (300 MHz, DMSO-d_6, δ): 9.8 (N*H*), 7.5 (aromatic protons *ortho* to NH), 7.3 (aromatic protons *meta* to NH), 6.3 (*H*C=), 2.7 (CH_2SH), 2.3 (COCH_2), 1.4–1.8 (COCH$_2$CH_2 and CH_2CH$_2$SH), 0.7–1.4 [(CH_2)$_6$]. ^{13}C NMR (75 MHz, DMSO-d_6, δ): 172.1 (*C*O), 140.3 (aromatic carbon attached to NH), 138.0 (HC=*C*Ph), 132.5 (aromatic carbon *para* to NH), 129.2 (aromatic carbons *meta* to NH), 119.2 (aromatic carbons *ortho* to NH), 116.1 (H*C* = CPh), 41.1 (*C*H$_2$CH$_2$SH), 36.8 (CO*C*H$_2$), 30.2, 29.4, 29.2, 29.0, 28.5, 28.2, 28.1 [(*C*H$_2$)$_6$], 25.6, 25.2 (COCH$_2$*C*H$_2$ and *C*H$_2$SH).

*P***2**. This polymer was obtained as a brown solid in 53.0% yield (Table 2, no. 4). M_w = 8200; M_w/M_n = 1.5. ^{1}H NMR (300 MHz, $CDCl_3$, δ): 6.0–8.0 (very weak, aromatic protons), 2.9 (CH_2S), 2.1–2.6 (COCH_2 and CH_3), 1.7 (CH_2CH$_2$S), 1.5 (COCH$_2$CH_2), 0.9–1.4 [(CH_2)$_6$]. ^{13}C NMR (75 MHz, $CDCl_3$, δ): 196.2 (*C*O), 37.3 (CO*C*H$_2$), 30.8 (*C*H$_2$S), 29.7, 29.5, 29.3, 29.2, 29.0, 28.6 [(*C*H$_2$)$_7$ and *C*H$_3$], 25.6 (COCH$_2$*C*H$_2$).

*P***3**. This polymer was obtained as a yellow solid in 83.0% yield (Table 3, no. 3). M_w = 15 800; M_w/M_n = 1.1. ^{1}H NMR (300 MHz, $CDCl_3$, δ): 7.4 (aromatic protons *ortho* to NH), 7.2 (aromatic protons *meta* to NH), 2.8 (SCH_2), 2.1–2.5 (CH_2CO and HC=CCH_2), 1.8 (CH_2CH$_2$CO), 1.7 (SCH$_2$CH_2), 1.6 (HC=CCH$_2$CH_2), 1.0–1.5 [HC=CCH$_2$CH$_2$(CH_2)$_4$ and SCH$_2$CH$_2$(CH_2)$_5$], 0.9 (CH_3). ^{13}C NMR (75 MHz, $CDCl_3$, δ): 172.7 (*C*O), 136.4 (HC=*C*), 133.0 (aromatic carbon attached to NH), 131.9 (aromatic carbon *para* to NH), 130.0 (aromatic carbons *meta* to NH), 121.2 (aromatic carbons *ortho* to NH), 119.5 (H*C* = C), 37.6 (S*C*H$_2$), 34.4 (*C*H$_2$CO), 31.8 (HC=C*C*H$_2$), 30.0, 29.4, 29.2, 29.0 [HC=CCH$_2$(*C*H$_2$)$_5$ and SCH$_2$(*C*H$_2$)$_5$], 26.3 (*C*H$_2$CH$_2$CO), 22.8 (*C*H$_2$CH$_3$), 14.1 (*C*H$_3$).

Preparation of ZnO Nanoparticles. Into a sample vial, 10 mL of equimolar (0.0125 M) aqueous solution of zinc nitrate [$Zn(NO_3)_2\cdot 6H_2O$] and hexamethyltetramine ($C_6H_{12}N_4$) was added. Then 0.2 mL dodecythiol was introduced into the solution and a two-phase system was formed. The vial was transferred to a preheated water bath, and the reaction mixture was kept at a constant temperature of 90 °C for 2 h. While the aqueous phase remained clear throughout the reaction, spongy cream-like solid formed in the dodecythiol layer, which turned white and became thicker as the reaction proceeded. The cream-like product in dodecythiol layer was collected and repeatedly washed with ethanol and deionized water and then filtered and dried in an oven at 90 °C for 4 h. The solid was calcined at 600 °C for 4 h to give a white powdery product. Its typical morphology is shown in Supporting Information, Figure S5, and its XRD pattern can be indexed to the wurtzite-type ZnO crystal JCPDS No. 36–1451 (Figure S6).

Preparations of P2/ZnO Hybrid and PPA/ZnO Blend. P**2** (20 mg), ZnO nanoparticles (1 mg), and THF (5 mL) were added into a tube and the mixture was stirred at room temperature for 24 h. The resultant hybrid was used directly. The blend of PPA and ZnO nanoparticles was prepared in a similar way.

Adsorption of ZnO Nanoparticles by Polymer Films. Thin films of P**1**-P**3** and PPA were cast from their solutions (3 mg/mL) in DCM on quartz plates. The polymer films were dipped perpendicularly into a suspension of ZnO nanoparticles (0.5 mg/mL) in ethanol for 1 h. The films were taken out from the suspension and washed with ethanol several times. PL and UV spectrometers were used to monitor and confirm that the ZnO nanoparticles unattached to the polymer films had been removed.

Acknowledgment. The work reported in this paper was partially supported by the National Science Foundation of China (Project Nos. 20634020, 50573065, and 50740460164), the Ministry of Science & Technology of China (Project No. 2002CB613401), and the Research Grants Council of Hong Kong (Project Nos. 602707, 602706, and HKU2/05C). B.Z.T. thanks the support from the Cao Guangbiao Foundation of Zhejiang University.

Supporting Information Available: TGA thermograms of P**1**−P**3** and PPA; absorption spectra of P**2**, ZnO, and their hybrid in THF; EDAX analysis results of the hybrid film; IR spectra of M**2** and P**2**; TEM image and XRD pattern of the ZnO nanoparticles. This material is available free of charge via the Internet at http://pubs.acs.org.

References and Notes

(1) (a) Huynh, W. U.; Dittme, J. J.; Alivisatos, A. P. *Science* **2002**, *295*, 2425–2427. (b) Beek, W. J. E.; Wienk, M. M.; Janssen, R. A. J. *Adv. Mater.* **2004**, *16*, 1009–1013. (c) Khanna, P. K.; Kulkarni, M. V.; Singh, N.; Lonkar, S. P.; Subbarao, V. V. V. S.; Viswanath, A. K. *Mater. Chem. Phys.* **2006**, *95*, 24–28. (d) Dridi, C.; Haouari, M.; Ouada, H. B.; Legrand, A. P.; Davenas, J.; Bernard, M.; Andre, J. J.; Said, A. H.; Mattoussi, F. *Mater. Sci. Eng., C* **2006**, *26*, 415–420. (e) Yang, C. H.; Bhongale, C. J.; Chou, C. H.; Yang, S. H.; Lo, C. N.; Chen, T. M.; Hsu, C. S. *Polymer* **2007**, *48*, 116–128. (f) Feng, X. M.; Huang, H. P.; Ye, Q. Q.; Zhu, J. J.; Hou, W. H. *J. Phys. Chem. C* **2007**, *111*, 8463–8468. (g) Khanna, P. K.; Lonkar, S. P.; Subbarao, V. V. V. S.; Jun, K. W. M. *Mater. Chem. Phys.* **2004**, *87*, 49–52. (h) Zotti, G.; Vercelli, B. *Chem. Mater.* **2006**, *18*, 3754–3763.

(2) (a) Cui, T. Y.; Zhang, J. H.; Wang, J. Y.; Cui, F.; Chen, W.; Xu, F. B.; Wang, Z.; Zhang, K.; Yang, B. *Adv. Funct. Mater.* **2005**, *15*, 481–486. (b) Yan, B.; Chen, D. R.; Jiao, X. L. *Mater. Res. Bull.* **2004**, *39*, 1655–1662. (c) Otsuka, H.; Akiyama, Y.; Nagasaki, Y.; Kataoka, K. *J. Am. Chem. Soc.* **2001**, *123*, 8226–8230. (d) Chen, X.; Yu, Z. T.; Chen, J. S.; Yang, B. *Mater. Lett.* **2004**, *58*, 384–386. (e) Bekiari, V.; Pagonis, K.; Bokias, G.; Lianos, P. *Langmuir* **2004**, *20*, 7972–7975. (f) Kim, B. J.; Bang, J.; Hawker, C. J.; Kramer, E. J. *Macromolecules*

2006, *39*, 4108–4114. (g) Koening, S.; Chechik, V. *Langmuir* **2006**, *22*, 5168–5173.
(3) (a) Lemon, B. I.; Crooks, R. M. *J. Am. Chem. Soc.* **2000**, *122*, 12886–12887. (b) Huang, B. H.; Tomalia, D. A. *J. Lumin.* **2005**, *111*, 215–223.
(4) (a) For reviews, see Lam, J. W. Y.; Tang, B. Z. *Acc. Chem. Res.* **2005**, *38*, 745–754. (b) Lam, J. W. Y.; Tang, B. Z. *J. Polym. Sci., Part A: Polym. Chem.* **2003**, *41*, 2607–2629.
(5) (a) Hua, J. L.; Li, Z.; Lam, J. W. Y.; Xu, H. P.; Sun, J. Z.; Dong, Y. P.; Dong, Y. Q.; Qin, A. J.; Yuan, W. Z.; Chen, H. Z.; Wang, M.; Tang, B. Z. *Macromolecules* **2005**, *38*, 8127–8130. (b) Xu, H. P.; Sun, J. Z.; Qin, A. J.; Hua, J. L.; Li, Z.; Dong, Y. Q.; Xu, H.; Yuan, W. Z.; Ma, Y. G.; Wang, M.; Tang, B. Z. *J. Phys. Chem. B* **2006**, *110*, 21701–21709. (c) Hua, J. L.; Lam, J. W. Y.; Li, Z.; Qin, A. J.; Sun, J. Z.; Dong, Y. Q.; Dong, Y. P.; Tang, B. Z. *J. Polym. Sci., Part A: Polym. Chem.* **2006**, *44*, 3538–3550. (d) Yuan, W. Z.; Sun, J. Z.; Dong, Y. Q.; Haussler, M.; Yang, F.; Xu, H. P.; Qin, A. J.; Lam, J. W. Y.; Zheng, Q.; Tang, B. Z. *Macromolecules* **2006**, *39*, 8011–8020.
(6) Xu, H. P.; Xie, B. Y.; Yuan, W. Z.; Sun, J. Z.; Yang, F.; Dong, Y. Q.; Qin, A. J.; Zhang, S.; Wang, M.; Tang, B. Z. *Chem. Commun.* **2007**, 1322–1324.
(7) (a) Sandstrom, P.; Boncheva, M.; Akerman, B. *Langmuir* **2003**, *19*, 7537–7543. (b) Levin, C. S.; Bishnoi, S. W.; Grady, N. K.; Halas, N. J. *Anal. Chem.* **2006**, *78*, 3277–3271. (c) Wuelfing, W. P.; Gross, S. M.; Miles, D. T.; Murray, R. W. *J. Am. Chem. Soc.* **1998**, *120*, 12696–12697. (d) Unsworth, L. D.; Sheardown, H.; Brash, J. L. *Langmuir* **2005**, *21*, 1036–1041.
(8) (a) Love, J. C.; Estroff, L. A.; Kriebel, J. K.; Nuzzo, R. G.; Whitesides, G. M. *Chem. Rev.* **2005**, *105*, 1103–1169, and references therein. (b) Lee, L. Y. S.; Lennox, R. B. *Langmuir* **2007**, *23*, 292–296. (c) Jiang, P.; Nion, A.; Marchenko, A.; Piot, L.; Fichou, D. *J. Am. Chem. Soc.* **2006**, *128*, 12390–12391.
(9) Chen, K. B.; Chen, M. H.; Yang, S. H.; Hsieh, C. H.; Hsu, C. S.; Chen, C. C.; Chien, H. J. *J. Polym. Sci., Part A: Polym. Chem.* **2006**, *44*, 5378–5390.
(10) (a) Morino, K.; Oobo, M.; Yashima, E. *Macromolecules* **2005**, *38*, 3461–3468. (b) Huang, K.; Tabata, M.; Mawatari, Y.; Miyasaka, A.; Sato, E.; Sadahiro, Y.; Kashiwaya, Y.; Ishiii, K. *J. Polym. Sci., Part A: Polym. Chem.* **2005**, *43*, 2836–2850.
(11) Xu, K. T.; Peng, H.; Lam, J. W. Y.; Poon, T. W. H.; Dong, Y. P.; Xu, H. Y.; Sun, Q. H.; Cheuk, K. K. L.; Salhi, F.; Lee, P. P. S.; Tang, B. Z. *Macromolecules* **2000**, *33*, 6918–6924.
(12) (a) Furlani, A.; Licoccia, S.; Russo, M. V. *J. Polym. Sci., Part A: Polym. Chem.* **1986**, *24*, 991–1005. (b) Yang, W.; Tabata, M.; Yokota, K.; Shimizu, A. *Polym. J.* **1991**, *23*, 1135–1138.
(13) (a) Xu, H.; Guang, S.; Zhang, S.; Tong, B.; Tang, B. Z. *Acta Polym. Sinica* **2001**, 186–190. (b) Sun, J.; Chen, H.; Xu, R.; Wang, M.; Lam, J. W. Y.; Tang, B. Z. *Chem. Commun.* **2002**, 1222–1223. (c) Li, B.; Cheuk, K. K. L.; Yang, D.; Lam, J. W. Y.; Wan, L.; Bai, C.; Tang, B. Z. *Macromolecules* **2003**, *36*, 5447–5450.
(14) (a) Nakazato, A.; Saeed, I.; Shiotsuki, M.; Sanda, F.; Masuda, T. *Macromolecules* **2004**, *37*, 4044–4047. (b) Lam, J. W. Y.; Dong, Y. P.; Cheuk, K. K. L.; Luo, J. D.; Xie, Z.; Kwok, H. S.; Mo, Z. S.; Tang, B. Z. *Macromolecules* **2002**, *35*, 1229–1240. (c) Hirao, K.; Ishii, Y.; Terao, T.; Kishimoto, Y.; Miyatake, T.; Ikariya, T.; Noyori, R. *Macromolecules* **1998**, *31*, 3405–3408. (d) Tang, B. Z.; Kong, X. X.; Wan, X. H.; Peng, H.; Lam, W. Y. *Macromolecules* **1998**, *31*, 2419–2432.
(15) (a) Lam, J. W. Y.; Dong, Y. P.; Cheuk, K. K. L.; Law, C. C. W.; Lai, L. M.; Tang, B. Z. *Macromolecules* **2004**, *37*, 6695–6704. (b) Kong, X.; Lam, J. W. Y.; Tang, B. Z. *Macromolecule* **1999**, *32*, 1722–1730.
(16) (a) Ye, C.; Xu, G. Q.; Yu, Z. Q.; Lam, J. W. Y.; Jang, J. H.; Peng, H. L.; Tu, Y. F.; Liu, Z. F.; Jeong, K. U.; Cheng, S. Z. D.; Chen, E. Q.; Tang, B. Z. *J. Am. Chem. Soc.* **2006**, *127*, 7668–7669. (b) Yu, Z. Q.; Liu, J. H.; Yan, J. J.; Liu, X. B.; Liang, D. H.; Lam, J. W. Y.; Dong, Y. P.; Li, Z. C.; Chen, E. Q.; Tang, B. Z. *Macromolecules* **2007**, *40*, 8342–8348.
(17) (a) Wegner, G. *Macromol. Chem. Phys.* **2003**, *204*, 347–357. (b) Laschewsky, A. *Adv. Polym. Sci.* **1995**, *124*, 1–86, and references therein. (c) Cochin, D.; Candau, F.; Zana, R.; Talmon, Y. *Macromolecules* **1992**, *25*, 4220–4223.
(18) (a) Yan, H. Q.; Johnson, J.; Law, M.; He, R. R.; Knutsen, K.; McKinney, J. R.; Pham, J.; Saykally, R.; Yang, P. D. *Adv. Mater.* **2003**, *15*, 1907–1911. (b) Pal, U.; Santiago, P. *J. Phys. Chem. B* **2005**, *109*, 15317–15321. (c) Shan, F. K.; Liu, G. X.; Lee, W. J.; Lee, G. H.; Kim, I. S.; Shinb, B. C. *Appl. Phys. Lett.* **2005**, *86*, 221910. (d) Watanabe, M.; Sakai, M.; Shibata, H.; Tampo, H.; Fons, P.; Iwata, K.; Yamada, A.; Matsubara, K.; Sakurai, K.; Ishizuka, S.; Niki, S.; Nakahara, K.; Takasu, H. *Appl. Phys. Lett.* **2005**, *86*, 221907. (e) Percec, V.; Aqad, E.; Peterca, M.; Rudick, J. G.; Lemon, L.; Ronda, J. C.; De, B. B.; Heiney, P. A.; Meijer, E. W. *J. Am. Chem. Soc.* **2006**, *128*, 16365–16372.
(19) (a) *Dictionary of Organometallic Compounds*, 2nd ed.; Chapman & Hall: London, 1995. (b) Schrock, R. R.; Osborn, J. A. *Inorg. Chem.* **1970**, *9*, 2339–2343.
(20) Tang, B. Z.; Poon, W. H.; Leung, S. M.; Leung, W. H.; Peng, H. *Macromolecules* **1997**, *30*, 2209–2212.

MA702337Z